

Fundamental Properties of the CH \cdots O Interaction: Is It a True Hydrogen Bond?

Yanliang Gu, Tapas Kar, and Steve Scheiner*

Contribution from the Department of Chemistry, Southern Illinois University, Carbondale, Illinois 62901-4409

Received June 1, 1999. Revised Manuscript Received August 5, 1999

Abstract: Ab initio calculations are used to analyze the CH \cdots O interaction between F $_n$ H $_{3-n}$ CH as proton donor and H $_2$ O, CH $_3$ OH, and H $_2$ CO as acceptor. The interaction is quite weak with CH $_4$ as donor but is enhanced by 1 kcal/mol with each F added to the donor. The CH \cdots O interaction behaves very much like a conventional OH \cdots O H-bond in most respects, including shifts in electron density that accompany the formation of the bond and the magnitudes of the various components of the interaction energy. The two sorts of H-bonds also gravitate toward a similar equilibrium geometry and are comparably sensitive to deformations from that structure. In a quantitative sense, while both CH \cdots O and OH \cdots O prefer a linear configuration, the former is somewhat more easily bent and is less sensitive to stretches from its equilibrium H-bond length. Whereas the OH bond has been shown to stretch and undergo a red shift in its vibrational frequency upon formation of a H-bond, the CH bond of the molecules studied here follows the opposite trend, a contraction and a blue shift. Analysis demonstrates that this opposite pattern is not due to any fundamental distinction between the two interactions, since the same sets of forces are acting on both. It is concluded that the CH \cdots O interaction can, indeed, be categorized as a true H-bond.

Introduction

The widespread occurrence and importance of hydrogen bonds have made them an active topic of research for many decades. Much has been learned about their fundamental properties from both experimental and theoretical perspectives.^{1,2} In their standard incarnation, H-bonds result from the approach of a proton donor molecule toward an acceptor, forming a bridge of the sort A–H \cdots B. The donor A atom is thought to be very electronegative, e.g., O or N, as is the acceptor atom B, which must also contain at least one lone pair of electrons by which to form the bridge.

Although carbon is not particularly electronegative, there were some early and intriguing suggestions that a C–H group could, nonetheless, form a H-bond under certain conditions.^{3,4} Support was later added to this idea on the basis of IR data^{5–7} and the geometry of molecular complexes in the gas phase^{8–10} and in crystalline environment.^{11,12} As the number of available crystal structures multiplied, so did the range of intermolecular contacts

that showed indications of some sort of CH \cdots O interaction.^{13–20} Geometric indications of such interactions are not limited to small molecules but have been extended to such important biological systems as nucleic acids,^{21–27} proteins,^{28–30} and carbohydrates.^{31–33} Moreover, these interactions do not necessarily disappear when the solid loses its regular structure, as CH \cdots O interactions can persist into the liquid phase.^{34,35}

* To whom correspondence should be addressed. E-mail: scheiner@chem.siu.edu.

(1) Jeffrey, G. A.; Saenger, W. *Hydrogen Bonding in Biological Structures*; Springer-Verlag: Berlin, 1991.

(2) Scheiner, S. *Hydrogen Bonding: A Theoretical Perspective*; Oxford University Press: New York, 1997.

(3) Glasstone, S. *Trans. Faraday Soc.* **1937**, *33*, 200.

(4) Dippy, J. F. J. *Chem. Rev.* **1939**, *25*, 151.

(5) Allerhand, A.; Schleyer, P. v. R. *J. Am. Chem. Soc.* **1963**, *85*, 1715.

(6) DeLaat, A. M.; Ault, B. S. *J. Am. Chem. Soc.* **1987**, *109*, 4232.

(7) Kariuki, B. M.; Harris, K. D. M.; Philp, D.; Robinson, J. M. A. *J. Am. Chem. Soc.* **1997**, *119*, 12679.

(8) Astrup, E. E.; Aomar, A. M. *Acta Chem. Scand.* **1975**, *A29*, 794.

(9) Peterson, K. I.; Klempner, W. *J. Chem. Phys.* **1984**, *81*, 3842.

(10) Fujii, A.; Fujimaki, E.; Ebata, T.; Mikami, N. *J. Am. Chem. Soc.* **1998**, *120*, 13256.

(11) Sutor, D. J. *J. Chem. Soc.* **1963**, 1105.

(12) Kaufmann, R.; Knöchel, A.; Kopf, J.; Oehler, J.; Rudolph, G. *Chem. Ber.* **1977**, *110*, 2249.

(13) Taylor, R.; Kennard, O. *J. Am. Chem. Soc.* **1982**, *104*, 5063.

(14) Desiraju, G. R. *Acc. Chem. Res.* **1991**, *24*, 290.

(15) Reetz, M. T.; Hütte, S.; Goddard, R. *J. Am. Chem. Soc.* **1993**, *115*, 9339.

(16) Song, J.-S.; Szalda, D. J.; Bullock, R. M. *J. Am. Chem. Soc.* **1996**, *118*, 11134.

(17) Pedireddi, V. R.; Chatterjee, S.; Ranganathan, A.; Rao, C. N. R. *J. Am. Chem. Soc.* **1997**, *119*, 10867.

(18) Desiraju, G. R. *Science* **1997**, *278*, 404.

(19) Harakas, G.; Vu, T.; Knobler, C. B.; Hawthorne, M. F. *J. Am. Chem. Soc.* **1998**, *120*, 6405.

(20) Kuduva, S. S.; Craig, D. C.; Nangia, A.; Desiraju, G. R. *J. Am. Chem. Soc.* **1999**, *121*, 1936.

(21) Auffinger, P.; Westhof, E. *Biophys. J.* **1996**, *71*, 940.

(22) Berger, I.; Egli, M.; Rich, A. *Proc. Nat. Acad. Sci. U.S.A.* **1996**, *93*, 12116.

(23) Wahl, M. C.; Rao, S. T.; Sundaralingam, M. *Nature Struct. Biol.* **1996**, *3*, 24.

(24) Egli, M.; Gessner, R. V. *Proc. Nat. Acad. Sci. U.S.A.* **1995**, *92*, 180.

(25) Metzger, S.; Lippert, B. *J. Am. Chem. Soc.* **1996**, *118*, 12467.

(26) Auffinger, P.; Westhof, E. *J. Mol. Biol.* **1997**, *274*, 54.

(27) Sigel, R. K. O.; Freisinger, E.; Metzger, S.; Lippert, B. *J. Am. Chem. Soc.* **1998**, *120*, 12000.

(28) Derewenda, Z. S.; Lee, L.; Derewenda, U. *J. Mol. Biol.* **1995**, *252*, 248.

(29) Bella, J.; Berman, H. M. *J. Mol. Biol.* **1996**, *264*, 734.

(30) Musah, R. A.; Jensen, G. M.; Rosenfeld, R. J.; McRee, D. E.; Goodin, D. B.; Bunte, S. W. *J. Am. Chem. Soc.* **1997**, *119*, 9083.

(31) Steiner, T.; Saenger, W. *J. Am. Chem. Soc.* **1992**, *114*, 10146.

(32) Steiner, T.; Saenger, W. *J. Am. Chem. Soc.* **1993**, *115*, 4540.

(33) Wahl, M. C.; Sundaralingam, M. *Trends Biochem. Sci.* **1997**, *22*, 97.

(34) Jedlovsky, P.; Turi, L. *J. Phys. Chem. B* **1997**, *101*, 5429.

The principle that a CH group can act as a proton donor in certain circumstances has been part of mainstream chemistry for many years. None would deny, for example, that HCN acts as a strong acid that can form a H-bond to a suitable acceptor.^{36,37} However, HCN is an exception; this idea becomes more questionable for most other CH proton donors. The alkyne group of acetylene, for example, may participate in interactions that resemble H-bonds in certain respects.^{9,38,39} The sp^3 hybridization of C in an alkane would normally be considered to make it less able to act as a proton donor,³¹ but alkanes appear capable of forming such interactions when sufficiently activated by neighboring electronegative substituents.^{40–42} There have even been hints from structural information that an unsubstituted alkane such as methane might act as a proton donor in certain extraordinary contexts.^{43,44}

While there is certainly abundant evidence that the CH and O groups approach one another with some regularity, the fundamental nature of the interaction remains an open question. That is, structural analysis may reveal the CH and O groups to be lined up in a configuration reminiscent of conventional H-bonds, but the inference does not necessarily follow that the interaction falls into the category of genuine H-bonds, or indeed that it is even attractive. Further complicating the situation, the $CH\cdots O$ interaction seldom occurs as the sole attractive force between two molecules but is much more commonly a secondary, and probably weaker, factor in the overall geometry of the crystal.

It is here that theoretical calculations can make a valuable contribution. One can compute the strength of a particular interaction in isolation from others, free of the complicating additional factors that contribute to the overall crystal structure. If an attractive force is identified, it can be dissected by quantum chemistry into its contributing factors, which can then be compared with the fingerprint of a true H-bond. One can answer the question of whether the $CH\cdots O$ interaction represents anything more than a simple electrostatic force between the partial negative charge on the oxygen and positive charge that accumulates on C–H. The intrinsic separation and preferred alignment can be assessed, as well as the sensitivity to deviations from ideal geometry. It is also possible to examine shifts of electron density that accompany the formation of a $CH\cdots O$ interaction, and thereby better understand its fundamental nature. Perhaps most importantly, calculations can be directed at a set of related complexes, designed so as to provide a systematic comparison of these putative H-bonds with more standard types.

Early calculations of relevant complexes applied a low level of theory, at least by the standards of today. The results indicated that $CH\cdots O$ interactions may, indeed, be attractive.^{45,46} The expected strengthening as a result of electronegative substituents and/or hybridization changes of the C atom was observed as

well.^{47–49} There were some crude estimates of the strength of the interaction, but these results varied widely.^{41,47} There have been a series of more accurate calculations of late,^{48–55} but these have not been systematic for the most part and have usually concerned themselves primarily with the interaction energy and not with the other important aspects of the interaction.

There still remain a number of important and fundamental questions that the present article is intended to address. How strong are $CH\cdots O$ interactions, and under what conditions might they be competitive with conventional H-bonds? Even if they are weaker, do the factors that contribute to the binding in $CH\cdots O$ fit the pattern of true H-bonds? H-bonds obey a characteristic pattern of sensitivity to stretches and bends from their optimal configuration; similar sensitivity on the part of $CH\cdots O$ interactions would add to the idea that they do, indeed, constitute true H-bonds. How do the nuclear and electronic changes that accompany the formation of the two sorts of interactions compare with one another? There has emerged in the recent literature some controversy as to whether the formation of a $CH\cdots O$ interaction causes changes in the CH stretching frequency and the equilibrium CH length that are opposite in sign to those observed in conventional H-bonds. Indeed, some have gone so far as to label $CH\cdots O$ interactions as “anti-H-bonds”.^{56–58} Another goal of this paper is to resolve this question and understand the underlying reason for any differences with conventional H-bonds.

Methods

The proton donor molecules considered here are methane and its fluorinated derivatives CFH_3 , CF_2H_2 , and CF_3H . Oxygen-containing proton acceptor molecules include the hydroxyl in H_2O and CH_3OH , as well as the carbonyl oxygen in H_2CO . The geometries of the various combinations are illustrated in Figure 1, where the important structural variables are defined. R refers to the distance between the C and O atoms. The nonlinearity of the putative H-bond is measured by α , the $\theta(HC\cdots O)$ angle. β represents the disposition of the HOY bisector with respect to the $C\cdots O$ axis in the case of H_2O and CH_3OH in Figure 1a but is defined in terms of the $C=O$ axis for H_2CO in Figure 1b. Most of the $CH\cdots O$ interactions are compared with the water dimer in Figure 1c, which is defined analogously to the parameters in Figure 1a.

Ab initio calculations were carried out using the Gaussian 94 and 98 sets of programs.^{59,60} Electron correlation was included in a number of ways, including second- and fourth-order Møller–Plesset perturbation theory (MP2, MP4),^{61–63} quadratic configuration interaction including

- (35) Mizuno, K.; Ochi, T.; Shindo, Y. *J. Chem. Phys.* **1998**, *109*, 9502.
 (36) Gutowsky, H. S.; Germann, T. C.; Augspurger, J. D.; Dykstra, C. E. *J. Chem. Phys.* **1992**, *96*, 5808.
 (37) Turi, L.; Dannenberg, J. J. *J. Phys. Chem.* **1993**, *97*, 7899.
 (38) Jeng, M.-L. H.; Ault, B. S. *J. Phys. Chem.* **1989**, *93*, 5426.
 (39) Steiner, T.; Lutz, B.; van der Maas, J.; Schreurs, A. M. M.; Kroon, J.; Tamm, M. *Chem. Commun.* **1998**, 171.
 (40) Green, R. D. *Hydrogen Bonding by C–H Groups*; Wiley-Interscience: New York, 1974.
 (41) Seiler, P.; Weisman, G. R.; Glendening, E. D.; Weinhold, F.; Johnson, V. B.; Dunitz, J. D. *Angew. Chem., Int. Ed. Engl.* **1987**, *26*, 1175.
 (42) Desiraju, G. R. *J. Chem. Soc., Chem. Commun.* **1989**, 179.
 (43) Davis, S. R.; Andrews, L. *J. Am. Chem. Soc.* **1987**, *109*, 4768.
 (44) Legon, A. C.; Roberts, B. P.; Wallwork, A. L. *Chem. Phys. Lett.* **1990**, *173*, 107.
 (45) Bonchev, D.; Cremaschi, P. *Theor. Chim. Acta* **1974**, *35*, 69.
 (46) Kollman, P.; McKelvey, J.; Johansson, A.; Rothenberg, S. *J. Am. Chem. Soc.* **1975**, *97*, 955.

- (47) Reynolds, C. H. *J. Am. Chem. Soc.* **1990**, *112*, 7903.
 (48) Turi, L.; Dannenberg, J. J. *J. Phys. Chem.* **1995**, *99*, 639.
 (49) Novoa, J. J.; Mota, F. *Chem. Phys. Lett.* **1997**, *266*, 23.
 (50) Tsuzuki, S.; Uchimar, T.; Tanabe, K.; Hirano, T. *J. Phys. Chem.* **1993**, *97*, 1346.
 (51) Vizioli, C.; de Azúa, M. C. R.; Giribet, C. G.; Contreras, R. H.; Turi, L.; Dannenberg, J. J.; Rae, I. D.; Weigold, J. A.; Malagoli, M.; Zanasi, R.; Lazzarotti, P. *J. Phys. Chem.* **1994**, *98*, 8858.
 (52) Erickson, J. A.; McLoughlin, J. I. *J. Org. Chem.* **1995**, *60*, 1626.
 (53) Alkorta, I.; Maluendes, S. *J. Phys. Chem.* **1995**, *99*, 6457.
 (54) Ornstein, R. L.; Zheng, Y. *J. Biomol. Struct. Dyn.* **1997**, *14*, 657.
 (55) Houk, K. N.; Menzer, S.; Newton, S. P.; Raymo, F. M.; Stoddart, J. F.; Williams, D. J. *J. Am. Chem. Soc.* **1999**, *121*, 1479.
 (56) Hobza, P.; Spirko, V.; Selzle, H. L.; Schlag, E. W. *J. Phys. Chem. A* **1998**, *102*, 2501.
 (57) Hobza, P.; Spirko, V.; Havlas, Z.; Buchhold, K.; Reimann, B.; Barth, H.-D.; Brutschy, B. *Chem. Phys. Lett.* **1999**, *299*, 180.
 (58) Hobza, P.; Havlas, Z. *Chem. Phys. Lett.* **1999**, *303*, 447.
 (59) Frisch, M. J.; Trucks, G. W.; Schlegel, H. B.; Gill, P. M. W.; Johnson, B. G.; Robb, M. A.; Cheeseman, J. R.; Keith, T. A.; Petersson, G. A.; Montgomery, J. A.; Raghavachari, K.; Al-Laham, M. A.; Zakrzewski, V. G.; Ortiz, J. V.; Foresman, J. B.; Cioslowski, J.; Stefanov, B. B.; Nanayakkara, A.; Challacombe, M.; Peng, C. Y.; Ayala, P. Y.; Chen, W.; Wong, M. W.; Andres, J. L.; Replogle, E. S.; Gomperts, R.; Martin, R. L.; Fox, D. J.; Binkley, J. S.; Defrees, D. J.; Stewart, J. J. P.; Head-Gordon, M.; Gonzalez, G.; Pople, J. A. *Gaussian 94*; Gaussian, Inc.: Pittsburgh, PA, 1995.

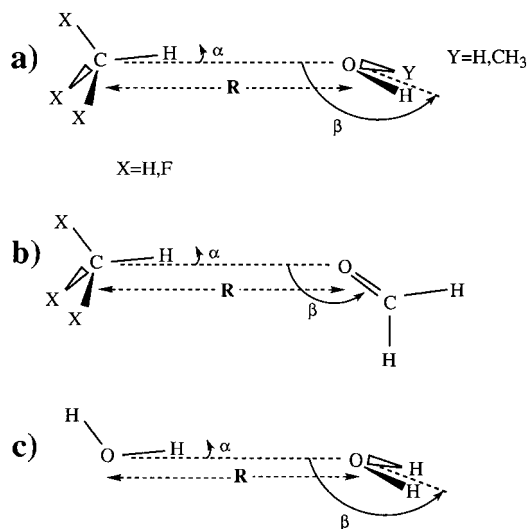


Figure 1. Geometries of systems investigated, defining geometrical parameters R , α , and β . X atoms in (a) and (b) may be H or F; Y can be H or CH₃.

singles and doubles (QCISD),⁶⁴ and coupled cluster at the singles and doubles levels with an extrapolation to triples, CCSD(T).^{65,66} Density functional methods (DFT) which include correlation were also examined, using the B3LYP functional.^{67,68}

Basis sets compared here are of the 6-31G and 6-311G varieties.⁶⁹⁻⁷¹ Diffuse functions were added to first-row atoms (+), and in some cases on H as well (++); single and double asterisks have a similar meaning with respect to polarization functions. Another basis set tested is Dunning's polarized correlation-consistent aug-cc-pVDZ set, augmented by diffuse functions.⁷² Interaction energies were computed as the difference in energy between the complex, on one hand, and the sum of isolated monomers, on the other hand. Basis set superposition error (BSSE) was corrected (where noted) by the counterpoise procedure of Boys and Bernardi.⁷³ Charges on individual atoms were computed using the natural population scheme.⁷⁴

Results

Energetics. The interaction energies of the various complexes, as computed at various levels and corrected for basis

(60) Frisch, M. J.; Trucks, G. W.; Schlegel, H. B.; Scuseria, G. E.; Robb, M. A.; Cheeseman, J. R.; Zakrzewski, V. G.; Montgomery, J. A.; Stratmann, R. E.; Burant, J. C.; Dapprich, S.; Millam, J. M.; Daniels, A. D.; Kudin, K. N.; Strain, M. C.; Farkas, O.; Tomasi, J.; Barone, V.; Cossi, M.; Cammi, R.; Mennucci, B.; Pomelli, C.; Adamo, C.; Clifford, S.; Ochterski, J.; Petersson, G. A.; Ayala, P. Y.; Cui, Q.; Morokuma, K.; Malick, D. K.; Rabuck, A. D.; Raghavachari, K.; Foresman, J. B.; Cioslowski, J.; Ortiz, J. V.; Stefanov, B. B.; Liu, G.; Liashenko, A.; Piskorz, P.; Komaromi, I.; Gomperts, R.; Martin, R. L.; Fox, D. J.; Keith, T.; Al-Laham, M. A.; Peng, C. Y.; Nanayakkara, A.; Gonzalez, C.; Challacombe, M.; Gill, P. M. W.; Johnson, B.; Chen, W.; Wong, M. W.; Andres, J. L.; Gonzalez, C.; Head-Gordon, M.; Replogle, E. S.; Pople, J. A. *Gaussian 98*, Revision A.6; Gaussian, Inc.: Pittsburgh, PA, 1998.

(61) Møller, C.; Plesset, M. S. *Phys. Rev.* **1934**, *46*, 618.

(62) Pople, J. A.; Seeger, R.; Krishnan, R. *Int. J. Quantum Chem., Quantum Chem. Symp.* **1977**, *11*, 149.

(63) Krishnan, R.; Pople, J. A. *Int. J. Quantum Chem.* **1978**, *14*, 91.

(64) Pople, J. A.; Head-Gordon, M.; Raghavachari, K. *J. Chem. Phys.* **1987**, *87*, 5968.

(65) Purvis, G. D.; Bartlett, R. J. *J. Chem. Phys.* **1982**, *76*, 1910.

(66) Scuseria, G. E.; Schaefer, H. F. *J. Chem. Phys.* **1989**, *90*, 3700.

(67) Becke, A. D. *J. Chem. Phys.* **1993**, *98*, 5648.

(68) Lee, C.; Yang, W.; Parr, R. G. *Phys. Rev. B* **1988**, *37*, 785.

(69) Hariharan, P. C.; Pople, J. A. *Theor. Chim. Acta* **1973**, *28*, 213.

(70) Krishnan, R.; Binkley, J. S.; Seeger, R.; Pople, J. A. *J. Chem. Phys.* **1980**, *72*, 650.

(71) Clark, T.; Chandrasekhar, J.; Spitznagel, G. W.; Schleyer, P. v. R. *J. Comput. Chem.* **1983**, *4*, 294.

(72) Woon, D. E.; Dunning, T. H. *J. Chem. Phys.* **1993**, *98*, 1358.

(73) Boys, S. F.; Bernardi, F. *Mol. Phys.* **1970**, *19*, 553.

(74) Reed, A. E.; Curtiss, L. A.; Weinhold, F. *Chem. Rev.* **1988**, *88*, 899.

set superposition error by the counterpoise procedure, are reported in Table 1. The first five rows of data refer to uncorrelated interaction energies, computed at the SCF level. Correlation is included first by the MP2 procedure, as well as by more complete methods, CCSD(T), MP4, and finally QCISD. The last two rows of data refer to DFT calculations which also include correlation.

In each case, the geometry was fully optimized at the indicated level with the single restriction of a linear H-bond, i.e., $\alpha = 0^\circ$. This restraint was imposed for a number of reasons. In the first place, a consistent geometry ensures a fair comparison between the strengths and natures of the different H-bonds. In the absence of such a restriction, some of the complexes optimized to geometries that are not relevant to this study. For example, suitable rotations of FH₂CH...OH₂ permit the F atom to come into contact with the protons of water, reversing the role of proton donor and acceptor and forming the more conventional H₃CF...HOH H-bond, quite different from the CH...O interaction desired for purposes of comparison. (The effects of relaxing this restriction are examined later in this report.)

The data in Table 1 indicate a surprising lack of sensitivity to basis set. At the SCF level for example, the interaction energies between CH₄ and OH₂ all lie in the narrow range of 0.16–0.21 kcal/mol. There is a tendency for aug-cc-pVDZ to predict slightly lower SCF interaction energies than the other basis sets, but the differences are not very large. The same insensitivity to basis set is evident in the correlated interaction energies as well. The MP2 values for FH₂CH...OH₂ all lie in the range between 1.2 and 1.3 kcal/mol, for example. This basis set insensitivity is consistent with a recent calculation of a closely related CH...O interaction.⁵⁸

Nor does there appear to be much difference between the various correlated methods. Using the 6-31+G** basis set as a common reference point, the MP2, MP4, QCISD, and CCSD(T) values of the interaction energies are remarkably uniform, varying among themselves by not more than 0.1 kcal/mol for any of the CH...O complexes. Indeed, even the DFT methods yield interaction energies quite similar to their ab initio counterparts. An earlier study found the MP2 method to very closely approximate MP4 data,⁵³ confirming our own data here. It is thus probably safe to conclude that the use of larger basis sets or more extensive inclusion of correlation would not perturb the values in Table 1 by a substantial margin.

Earlier estimates of the binding energy for the weakest of these complexes, between CH₄ and OH₂, vary between 0.3 and 0.7 kcal/mol,^{49,75,76} comparable to the correlated values derived here, as is the interaction energy for H₃CH...OCH₂ quite close to a literature value of 0.5 kcal/mol.⁷⁷ The smaller value derived here can be attributed to the use of a basis set without polarization functions of higher angular quantum numbers, needed to saturate the dispersion attraction.

Summarizing the best estimates of the energetics contained in Table 1, there is a clear progression toward stronger interactions as F atoms are added to the proton donor. The interaction energy of CH₄ with OH₂ is about 0.3 kcal/mol, whereas those of FH₂CH...OH₂ and F₂HCH...OH₂ are respectively 1.3 and 2.3 kcal/mol, an increment of about 1.0 kcal/mol for each F atom. This increment is essentially identical to that computed earlier for the same collection of systems.⁵³ It is further supported by a MP2/6-31+G** value of 3.7 kcal/mol

(75) Woon, D. E.; Zeng, P.; Beck, D. R. *J. Chem. Phys.* **1990**, *93*, 7808.

(76) Szczesniak, M. M.; Chalasinski, G.; Cybulski, S. M.; Cieplak, P. *J. Chem. Phys.* **1993**, *98*, 3078.

(77) Novoa, J. J.; Lafuente, P.; Mota, F. *Chem. Phys. Lett.* **1998**, *290*, 519.

Table 1. Interaction Energies (kcal/mol) Calculated with Counterpoise Correction of Basis Set Superposition Error^a

		H ₃ CH...			FH ₂ CH...			F ₂ HCH...			HOH...OH ₂
		OH ₂	CH ₃ OH	H ₂ CO	OH ₂	CH ₃ OH	H ₂ CO	OH ₂	CH ₃ OH	H ₂ CO	
SCF	6-31+G*	0.21	0.20	0.15	1.40	1.10	0.99	2.23	2.25	1.95	4.17
	6-31+G**	0.21	0.22	0.16	1.14	1.14	1.03	2.28	2.32	2.01	4.21
	6-31++G**	0.21	0.22	0.16	1.15	1.13	1.02	2.27	2.31	1.99	4.20
	6-311+G**	0.20	0.22	0.17	1.11	1.12	1.02	2.23	2.29	1.99	4.10
	aug-cc-pVDZ	0.16	0.16	0.14	0.89	0.89	0.90	1.85	1.89	1.79	3.53
MP2	6-31+G*	0.24	0.37	0.35	1.33	1.47	1.21	2.57	2.80	2.12	4.61
	6-31+G**	0.29	0.43	0.37	1.34	1.51	1.21	2.53	2.78	2.11	4.51
	6-31++G**	0.30	0.43	0.37	1.34	1.51	1.21	2.53	2.78	2.09	4.56
	6-311+G**	0.35	0.50	0.38	1.28	1.44	1.13	2.34	2.58	1.93	4.30
	aug-cc-pVDZ	0.43	0.63	0.46	1.23	1.42	1.20	2.24	2.52	2.04	4.11
CCSD(T)	6-31+G**	0.29		0.35	1.32		1.21	2.50		2.13	4.36
MP4 ^b	6-31+G**	0.29	0.43	0.37	1.31	1.48	1.21	2.47	2.72	2.09	4.34
QCISD ^b	6-31+G**	0.23	0.34	0.31	1.26	1.41	1.18	2.45	2.67	2.12	4.25
B3LYP	6-31+G**	0.25	0.29	0.13	1.32	1.30	0.95	2.45	2.55	1.85	4.80
	6-311+G**	0.26	0.30	0.14	1.28	1.34	0.97	2.48	2.63	1.89	4.77

^a All geometries were fully optimized at the level indicated, with the single restriction of a linear CH...O. ^b Using MP2/6-31+G** geometry.

Table 2. Optimized Intermolecular R(C...O) Distances (Å) with CH...O Held Linear

		H ₃ CH...			FH ₂ CH...			F ₂ HCH...			HOH...OH ₂
		OH ₂	CH ₃ OH	H ₂ CO	OH ₂	CH ₃ OH	H ₂ CO	OH ₂	CH ₃ OH	H ₂ CO	
SCF	6-31+G*	4.051	4.067	4.144	3.642	3.669	3.771	3.455	3.460	3.568	2.980
	6-31+G**	3.963	4.008	4.089	3.637	3.644	3.736	3.462	3.455	3.547	2.999
	6-31++G**	3.944	4.008	4.089	3.637	3.658	3.738	3.466	3.466	3.547	2.999
	6-311+G**	3.931	4.008	4.122	3.666	3.688	3.753	3.492	3.484	3.555	3.002
	aug-cc-pVDZ	4.163	4.180	4.201	3.803	3.797	3.804	3.589	3.571	3.602	3.052
MP2	6-31+G*	3.587	3.587	3.805	3.437	3.427	3.595	3.317	3.296	3.444	2.921
	6-31+G**	3.592	3.582	3.777	3.456	3.436	3.575	3.337	3.310	3.437	2.927
	6-31++G**	3.596	3.582	3.777	3.458	3.436	3.577	3.336	3.304	3.436	2.925
	6-311+G**	3.649	3.642	3.784	3.511	3.485	3.614	3.379	3.347	3.475	2.924
	aug-cc-pVDZ	3.771	3.674	3.771	3.589	3.536	3.589	3.434	3.380	3.451	2.957
CCSD(T)	6-31+G**	3.599		3.777	3.461		3.593	3.343		3.439	2.939
B3LYP	6-31+G**	3.675	3.726	3.953	3.494	3.501	3.651	3.358	3.349	3.481	2.905
	6-311+G**	3.674	3.716	3.950	3.492	3.494	3.628	3.354	3.339	3.464	2.908

for F₃CH...OH₂, virtually identical to a recent calculation of the interaction between F₃CH and ethylene oxide (similar to water), which yielded an interaction energy of 3.76 kcal/mol at a comparable level of theory,⁵⁸ about 1.2 kcal/mol higher than the difluorinated proton donors. This increment can be compared with the same sort of quantity computed for Cl substituents, albeit at a lower level of theory, where each additional Cl atom added 1–2 kcal/mol to the interaction energy.⁷⁸

With regard to the particular proton acceptor molecule, there appears to be a very small increase of perhaps 0.1–0.2 kcal/mol as a result of replacing one of water's H atoms by a methyl group. The effect of changing oxygen's formal hybridization from the sp³ of water to the sp² of H₂CO is variable. There is no obvious effect at all with methane. However, in the more strongly bound complexes, carbonyl would appear to be a slightly weaker proton acceptor than is hydroxyl. The binding energy of H₂CO is less than that of H₂O by 0.1 for proton donor FH₂CH and is smaller by perhaps 0.4 kcal/mol for the stronger donor F₂HCH. The much greater sensitivity of binding energy to the nature of the proton donor as compared to the acceptor agrees with findings from crystal structural data.⁷⁹

One final point concerning the energetics is the contribution made by electron correlation. The difference between SCF and MP2 interaction energies is rather small. This correlation component amounts to some 0.1–0.3 kcal/mol for the various complexes with H₂O or H₂CO. This contribution is somewhat higher for the complexes with methanol, suggesting that the higher complexation energy might be due, in part, to the added

dispersion energy (akin to London force) that is associated with a larger acceptor molecule (vide infra).

The last column of Table 1 reports analogous energetic data for the water dimer, the classic paradigm of hydrogen bonding. The binding energy is considerably larger than that of the difluorinated F₂HCH...OH₂, by more than a factor of 2, and exceeds the comparable value for F₃CH...OH₂ by 1.0 kcal/mol. Although the CH...O interactions are weaker than the conventional H-bond, they all share the same small correlation component.

It is worth stressing that failure to correct the BSSE would have resulted in erroneous conclusions. These superposition errors are fairly small at the SCF level, less than 0.3 kcal/mol for the CH...O interactions. However, due to the weakness of the interactions involving methane, the computed superposition errors of 0.1 kcal/mol are comparable to the true SCF interaction energy. The BSSE is larger for the conventional H-bond of the water dimer, approaching 1.0 kcal/mol with the 6-31+G* basis set. The BSSE is several times larger at the correlated levels. In the case of the complexes containing methane, for example, the BSSE can be as much as 2 or 3 times larger than the corrected interaction energy. Taking the more strongly bound F₂HCH...OH₂ as another example, the correlated BSSEs are on the order of 1.0 kcal/mol; they climb to as much as 2 kcal/mol for the water dimer.

Geometries. The equilibrium intermolecular separations are listed in Table 2, which again correspond to optimized structures with C–H...O held linear. As in the case of the binding energies in Table 1, these distances are fairly insensitive to details of the basis set. Taking CH₄...OH₂ as an example again, whereas

(78) Hobza, P.; Sandorfy, C. *Can. J. Chem.* **1984**, *62*, 606.

(79) Steiner, T. *J. Chem. Soc., Chem. Commun.* **1994**, 2341.

Table 3. Change in CH Bond Length (mÅ) of Proton Donor Caused by Complexation, with CH...O Held Linear^a

	H ₃ CH... ^a			FH ₂ CH... ^a			F ₂ HCH... ^a			F ₃ CH... ^a			HOH...OH ₂
	OH ₂	CH ₃ OH	H ₂ CO	OH ₂	CH ₃ OH	H ₂ CO	OH ₂	CH ₃ OH	H ₂ CO	OH ₂	CH ₃ OH	H ₂ CO	
SCF	-0.6	-0.5	-0.5	-1.9	-1.8	-1.8	-2.8	-2.7	-2.7	-2.6	-2.3	-2.9	4.2
MP2	-0.5	-0.2	-0.4	-1.7	-1.4	-1.5	-2.7	-2.4	-2.5	-2.3	-1.8	-2.6	5.2

^a Results were computed with the 6-311+G** basis set.**Table 4.** Change in Bond Length (mÅ) of Proton Acceptor Caused by Complexation, with CH...O Held Linear^a

	H ₃ CH... ^a			FH ₂ CH... ^a			F ₂ HCH... ^a			F ₃ CH... ^a			HOH...OH ₂ , r(OH)
	OH ₂ , r(OH)	CH ₃ OH, r(CO)	H ₂ CO, r(CO)	OH ₂ , r(OH)	CH ₃ OH, r(CO)	H ₂ CO, r(CO)	OH ₂ , r(OH)	CH ₃ OH, r(CO)	H ₂ CO, r(CO)	OH ₂ , r(OH)	CH ₃ OH, r(CO)	H ₂ CO, r(CO)	
SCF	0.0	0.4	0.2	0.2	1.8	0.8	0.4	3.5	1.4	0.6	5.1	2.1	0.4
MP2	0.4	0.2	0.1	0.6	1.5	0.4	0.7	2.9	0.7	0.8	4.3	1.0	0.4

^a Results were computed with the 6-311+G** basis set.

its SCF complexation energies vary between 0.16 and 0.21 kcal/mol, the $R(\text{C}\cdots\text{O})$ distances lie in the 3.93–4.16 Å range. There is even less variance in the equilibrium separation for the more strongly bound complexes. F₂HCH...OH₂, for example, has SCF distances between 3.455 and 3.589 Å. The correlated separations are likewise well clustered for each complex considered, and the MP2 values are consonant with the distances computed with CCSD(T). In most cases, the DFT intermolecular separations mimic the ab initio correlated values, with an exception of slight overestimates in the case of the very weakly bound complexes containing CH₄.

Just as the addition of each F atom to the proton donor molecule adds about 1 kcal/mol to the binding energy, there appears to be a corresponding progressive contraction of about 0.10–0.15 Å in $R(\text{C}\cdots\text{O})$. The latter separation varies from a maximum of about 3.6–3.7 Å for H₃CH...OH₂ down to 3.3–3.4 Å for the doubly fluorosubstituted F₂HCH...OH₂, and 3.248 Å for F₃CH...OH₂. Even this distance is longer than the 2.9–3.0 Å O...O separation in the water dimer, consistent with the lower binding energy of the former. This range of intermolecular distances for CH...O contacts coincides nicely with X-ray crystal structures,⁴² where each successive replacement of a H atom by Cl was found to lead to a shortening of the intermolecular separation.

It was noted above that replacing a hydrogen atom of the proton acceptor by a methyl group adds a small increment to the binding energy. This effect is observed only at the correlated level, as the SCF binding energies of OH₂ and CH₃OH are virtually identical. The same may be said for the equilibrium separations. Whereas the SCF values of $R(\text{C}\cdots\text{O})$ are very similar, there is a clearly closer approach in the case of CH₃-OH at the correlated level. This fact adds support to the contention that the methyl group's contribution to the binding is largely a dispersion-related phenomenon. The lesser ability of the carbonyl oxygen to act as proton acceptor, relative to water, is evident also in the longer intermolecular separations for H₂CO. Finally, just as electron correlation added a small component to the interaction energies of all the complexes, so too are the equilibrium separations reduced at the correlated level.

One of the characteristic markers of traditional hydrogen bonding is the stretch that it causes in the X–H bond of the proton donor molecule. The changes in the optimized C–H bond length that occur in the various complexes, relative to the isolated pertinent single molecule, are reported in Table 3. The data there correspond to the 6-311+G** basis set, but the changes in bond length are rather insensitive to basis set, as are the geometries themselves. It is worth stressing that the

perturbations are reported in milliångstroms, as they are rather small. More importantly, all of the changes in C–H bond length are negative in sign; i.e., this bond contracts as a result of complexation. This change is contrary to the pattern in conventional H-bonds, where the bond undergoes a stretch, as illustrated by the last column for the water dimer.

A scan of the data in Table 3 illustrates that the amount of the C–H bond contraction is roughly correlated with the strength of the interaction. The amount of the bond length reduction generally increases as the proton donor becomes stronger, i.e., H₃CH < FH₂CH < F₂HCH; however, the geometry changes in the trifluorosubstituted F₃CH show no further increase over its predecessor, F₂HCH. The nature of the proton acceptor does not appear to matter much. It is also worth noting that correlation does not substantially change the bond contractions, reducing this quantity by only a very small amount, so one can conclude that the fundamental cause of the bond contraction is associated with the SCF level. Comparison with the last column illustrates that the C–H contractions in these CH...O complexes remain smaller in magnitude than the O–H stretch in the water dimer, obeying the same trend as the interaction energies in Table 1. A number of recent calculations have confirmed the contraction of the C–H bond,^{80–82} as, for example, when F₃CH forms a complex with ethylene oxide,⁵⁸ where the degree of bond shortening is comparable to those reported here.

The effects of the formation of the complexes upon the geometry of the proton acceptor molecule are displayed in Table 4. The quantities reported refer to the bond between the proton-accepting O atom and the atom to which it is bonded within the acceptor molecule. In general, all of these bonds show a slight lengthening, and the amount of this stretch scales approximately with the strength of the interaction. Perusal of the data indicates that the O–H bonds of the water molecule do not stretch by much, less than 1 mÅ in all cases. The CO bonds of CH₃OH and H₂CO are more susceptible to lengthening, particularly the single bond of the former. This bond stretches as much as 4–5 mÅ in the case of F₃CH...OHCH₃. The effects of correlation upon these stretches are not consistent; in the complexes involving water, the MP2 lengthenings are greater than the SCF values, while the reverse is true for CH₃OH and H₂CO. The stretches that occur in the water acceptor molecule are 0.4 mÅ in the case of the conventional H-bond of HOH...OH₂, not much different in sign or magnitude than those for CH...O interactions.

(80) Yoshida, H.; Harada, T.; Murase, T.; Ohno, K.; Matsuura, H. *J. Phys. Chem. A* **1997**, *101*, 1731.(81) Masella, M.; Flament, J.-P. *J. Chem. Phys.* **1999**, *110*, 7245.(82) Wu, D. Y.; Ren, Y.; Wang, X.; Tian, A. M.; Wong, N. B.; Li, W.-K. *J. Mol. Struct. (THEOCHEM)* **1999**, *459*, 171.

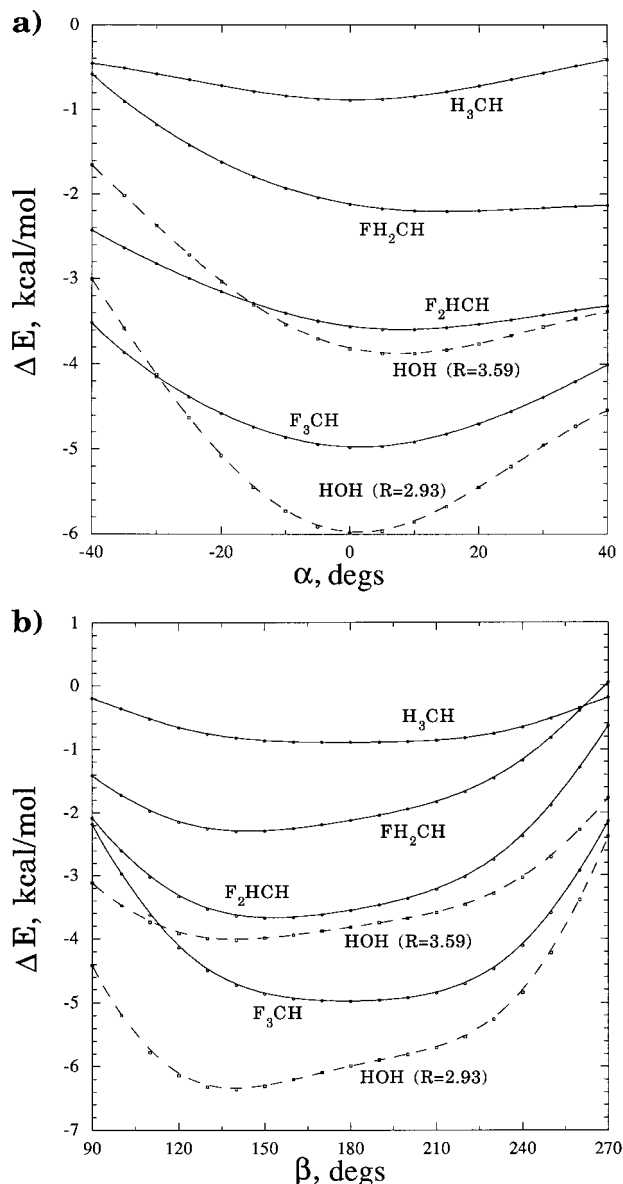


Figure 2. Interaction energies as a function of (a) $\alpha = \theta(HC \cdots O)$, where 0° refers to a linear $C-H \cdots O$ arrangement, and (b) β (see Figure 1). Energies were calculated at the MP2/6-31+G** level and are uncorrected for BSSE. Each curve is labeled with the identity of the proton donor molecule; the acceptor is water in each case. Broken curves refer to water dimer, both at its equilibrium $O \cdots O$ separation (2.927 Å) and at the intermolecular distance of the $H_3CH \cdots OH_2$ system (3.592 Å). Positive values of α rotate the proton donor molecule in such a way that any F substituents come closer to the water acceptor.

Sensitivity to Distortion. Hydrogen bonds are distinguished from generalized electrostatic interactions by their directional character. For example, there is a tendency of $O-H \cdots O$ toward linearity. The question as to whether $C-H \cdots O$ interactions are likewise highly dependent upon the angular aspects of the geometry remains a source of controversy.^{83,84}

The directionality of the $C-H \cdots O$ interactions is illustrated by the solid curves in Figure 2a, where they may be compared with the conventional H-bond of the water dimer (broken curves). The optimal value of α for the $H_3CH \cdots OH_2$ complex is 0° , as it is for $F_3CH \cdots OH_2$. The equilibrium α angles are slightly larger than 0° when one or two F atoms are added to

the proton donor, reflecting a certain amount of attraction between these F substituents and the H atoms of the water molecule. However, these equilibrium values are displaced only a small amount from 0° , 10° or less, so we may conclude that the $C-H \cdots O$ interactions tend toward linearity, as do conventional H-bonds.

The broken curves in Figure 2a illustrate the same sort of angular dependence in the water dimer. The lower of these two curves corresponds to the optimum $R(O \cdots O)$ distance of 2.927 Å. Since this is closer than the contacts in the $CH \cdots O$ systems, the upper broken curve was calculated, which represents the equivalent energetics for the water dimer, but with $R(O \cdots O)$ set equal to that in the $H_3CH \cdots OH_2$ complex, 3.592 Å. It may first be noted that the optimum value of α in the latter case is $5-10^\circ$ for the water dimer, quite close to the minimum in the $F_2HCH \cdots OH_2$ curve with which it intersects. Most importantly, even though these two curves have a comparable interaction energy of 3.5–4.0 kcal/mol, the one corresponding to the $CH \cdots O$ system is clearly flatter. For example, a shift of α by $\pm 20^\circ$ from its equilibrium value destabilizes the $CH \cdots O$ system by only about 0.2 kcal/mol, while the deformation energy of the water dimer for the same 20° distortion is roughly twice this amount. The dependence of the interaction energy upon nonlinearity α is even smaller for the weaker complexes, $H_3CH \cdots OH_2$ and $FH_2CH \cdots OH_2$. Whereas the trifluorinated $F_3CH \cdots OH_2$ complex is of comparable binding energy to the equilibrium water dimer, its corresponding solid curve is clearly flatter than the broken curve just below it. We conclude that $C-H \cdots O$ interactions have the same tendency toward linearity as conventional H-bonds but are less sensitive to angular deformations.

This trend toward linearity is consistent with findings in crystals and small molecules,^{85,86} as is the “softer” directionality in these weaker interactions.^{83,84} Why then are many $\alpha(C-H \cdots O)$ angles larger than their $\alpha(O-H \cdots O)$ counterparts? The reason may lie simply in the lesser energetic cost needed to distort the former from their preferred linearity. The other constraints imposed on the molecular contacts by the remainder of the crystal or supermolecular forces may more easily bend these $\alpha(C-H \cdots O)$ angles.

Surveys of $C-H \cdots O$ interactions in a set of proteins and organic molecules have revealed a tendency for the bridging hydrogen to approach the oxygen close to the plane of its two lone pairs,^{13,28} and within that plane, toward one lone pair or the other.^{83,87} It is thus of interest to contrast the two sorts of H-bonds with respect to the angular aspects of the proton acceptor. The curves in Figure 2b represent the analogous quantities as in Figure 2a, except that the angle being altered is β , between the $C \cdots O$ axis and the bisector of the water molecule. The preferred value of β in the $H_3CH \cdots OH_2$ and $F_3CH \cdots OH_2$ systems is 180° , but this angle shifts about 30° toward smaller values as one or two F atoms are added to the proton donor. As in the earlier case, this shift reflects the attraction between the latter fluorines and the H atoms of the water. It is most notable that the curves that lie close together, representing $F_2HCH \cdots OH_2$ and the water dimer with $R = 3.592$ Å, are nearly parallel to one another. In other words, there is no significant difference in the sensitivity of the energy to the orientation of the proton acceptor molecule between a $CH \cdots O$ and a conventional H-bond.

(85) Steiner, T. *Chem. Commun.* **1997**, 727.

(86) van de Bovenkamp, J.; Matxain, J. M.; van Duijneveldt, F. B.; Steiner, T. *J. Phys. Chem. A* **1999**, *103*, 2784.

(87) Braga, D.; Grepioni, F.; Biradha, K.; Pedireddi, V. R.; Desiraju, G. R. *J. Am. Chem. Soc.* **1995**, *117*, 3156.

(83) Steiner, T.; Kanters, J. A.; Kroon, J. *Chem. Commun.* **1996**, 1277.

(84) Brandl, M.; Lindauer, K.; Meyer, M.; Sühnel, J. *Theor. Chim. Acta* **1999**, *101*, 103.

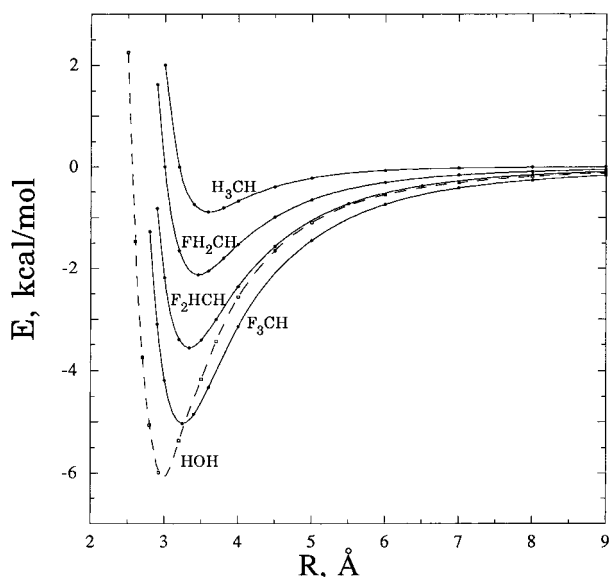


Figure 3. Interaction energies as a function of intermolecular separation $R(\text{O}/\text{C}\cdots\text{O})$. Energies were calculated at the MP2/6-31+G** level and are uncorrected for BSSE. Each curve is labeled with the identity of the proton donor molecule; the acceptor is water in each case. Broken curve refers to the water dimer.

While the particular level of calculation presented in Figure 2 incorporates electron correlation via the computationally efficient MP2 procedure, higher levels of theory were considered as well. All correlated calculations, MP4, CCSD(T), and QCISD, showed a sensitivity of the interaction energy to angular aspects of the H-bond that is virtually identical to the MP2 curves of Figure 2.

In addition to the angular aspects of the two sorts of H-bonds, there is also the question as to how quickly the attractive nature of the interaction dies off with distance. This question is addressed in Figure 3, which illustrates as a broken curve the binding energy for the water dimer as a function of the interoxygen separation. The four solid curves represent the same property for the indicated CH...O interactions, all with water as the proton acceptor molecule. It is, of course, no surprise that the minimum in the water dimer is deeper than those of the four CH...O systems, according to the energetic data in Table 1.

What is more interesting is the observation that this weaker sort of CH...O interaction dies off more slowly with distance than does the conventional H-bond of the water dimer. Compare, for example, the water dimer with $\text{F}_2\text{HCH}\cdots\text{OH}_2$. While the curve for the former is some 50% deeper than the latter at their minima, the binding energies of the two systems are virtually indistinguishable for distances of 4 Å and longer. That is, the weaker $\text{F}_2\text{HCH}\cdots\text{OH}_2$ interaction is every bit as strong as $\text{OH}\cdots\text{O}$ for distances longer than the equilibrium contact. From a more quantitative perspective, a stretch of the water dimer by 1 Å from its equilibrium length reduces the interaction energy to 40% of its maximum value, from 6 to 2.5 kcal/mol. A stretch of the $\text{F}_2\text{HCH}\cdots\text{OH}_2$ by the same 1 Å retains about 55% of the maximum interaction energy of 3.5 kcal/mol. The more gradual reduction of interaction energy for the CH...O bond is even more obvious for the case of $\text{F}_3\text{CH}\cdots\text{OH}_2$. The minimum in this potential lies at about 5 kcal/mol, as compared to 6 for the water dimer. But once the two subunits begin to move away from one another, the curves cross one another. As a result, the interaction energy for $\text{F}_3\text{CH}\cdots\text{OH}_2$ is more attractive than it is for the water dimer for all separations greater than about 3.3 Å.

Table 5. Shift in Frequency and Intensity of Antisymmetric C–H Stretch in Proton Donor Caused by Complexation, with CH...O Held Linear^a

	$\Delta\nu, \text{cm}^{-1}$			I/I_0^b		
	OH_2	CH_3OH	H_2CO	OH_2	CH_3OH	H_2CO
$\text{H}_3\text{CH}\cdots$	10	5	7	0.07	0.05	0.24
$\text{FH}_2\text{CH}\cdots$	22	17	19	0.09	0.09	0.18
$\text{F}_2\text{HCH}\cdots$	26	20	24	0.16	0.20	0.19
$\text{F}_3\text{CH}\cdots$	42	47	20	0.70	0.68	0.83
$\text{HOH}\cdots$	–31			1.89		

^a Results were computed at the MP2/6-31+G** level. ^b Ratio of intensity in the complex/isolated subunit.

In summary, then, the CH...O interaction tends to be weaker than a conventional H-bond, and both tend toward a linear arrangement. However, the CH...O system is less sensitive to deviations from linearity and also tends to retain its binding character over longer ranges of intermolecular separation.

Vibrational Spectra. Another characteristic feature of conventional hydrogen bonds concerns their vibrational spectrum. The frequency associated with the O–H stretch is typically red-shifted, and at the same time its intensity is enhanced, upon formation of a H-bond. Taking the water dimer as an example, a MP2/6-31+G** calculation leads to a decrease in the OH stretching frequency of the proton donor (specifically, the bond involving the bridging hydrogen) by 31 cm^{-1} , as indicated by the negative value in Table 5. The last row of the table indicates that the intensity of this mode in the complex is greater than that in the monomer by a factor of 1.89. These trends contrast vividly with the other complexes involving a CH bond as the proton donor. Note that all the other complexes have shifts of the C–H stretching frequency of positive sign, i.e., a blue shift. Such shifts are supported by a number of experimental observations.^{35,57,88,89} Likewise, instead of the intensity magnification that arises in the conventional H-bond of the water dimer, the C–H stretches all suffer a reduced intensity in the complex.

More specifically, the blue shifts of the CH bond in CH_4 are predicted to be in the range of 5–10 cm^{-1} . These shifts are progressively larger for single, double, and then triple fluoro-substitution, reaching a peak of 47 cm^{-1} for $\text{F}_3\text{CH}\cdots\text{OHCH}_3$, even larger than the red shift in the water dimer, although this CH...O interaction is not quite as strong as that in the latter complex. Another study found a similarly large blue shift when F_3CH is paired with ethylene oxide.⁵⁸

The decreases in the intensity of the C–H stretch caused by complex formation are contained in the right half of Table 5. The patterns here are not as clear as those above. There is a general trend for the weakest interactions to produce the greatest reduction in intensity in the cases of OH_2 and OHCH_3 . For example, the intensity of this stretch in $\text{H}_3\text{CH}\cdots\text{OH}_2$ is only 7% of that in isolated CH_4 , whereas the same quantity rises progressively with fluorine substitution until it reaches 70% in the more strongly bound complex of water with F_3CH . When H_2CO acts as the proton acceptor, on the other hand, there is no clear correlation at all between the strength of the interaction and the intensity loss. The only fully unambiguous observation is that all of the CH...O interactions result in a loss of intensity in the CH stretching mode, relative to the monomer, in opposition to the intensity enhancement characteristic of conventional H-bonds.

Electron Density Shifts. An important window into the fundamental nature of a molecular interaction such as the

(88) Chaney, J. D.; Goss, C. R.; Folting, K.; Santarsiero, B. D.; Hollingsworth, M. D. *J. Am. Chem. Soc.* **1996**, *118*, 9432.

(89) Bedell, B. L.; Goldfarb, L.; Mysak, E. R.; Samet, C.; Maynard, A. *J. Phys. Chem. A* **1999**, *103*, 4572.

Table 6. Dipole Moment of Complex Relative to Monomers and Charge Transferred from Proton Acceptor to Donor Molecule^a

	$\Delta\mu_z$, ^b D			CT, ^c me		
	OH ₂	CH ₃ OH	H ₂ CO	OH ₂	CH ₃ OH	H ₂ CO
H ₃ CH...	0.217	0.265	0.209	4	4	2
FH ₂ CH...	0.277	0.367	0.331	6	7	3
F ₂ HCH...	0.336	0.458	0.442	8	10	6
F ₃ CH...	0.405	0.572	0.566	11	14	8
HOH...	0.409			13		

^a Results were computed at the MP2/6-31+G** level. ^b $\Delta\mu_z$, defined as difference between dipole moment of complex and the vector sum of the dipoles of the isolated monomers (in the geometries adopted in the complex), all along the C—H...O direction. ^c Charge transfer (CT) defined as sum of atomic charges on the proton acceptor molecule.

C—H...O bond can be opened by studying shifts in electron density that accompany formation of the bond. One means of quantifying this shift is via the overall dipole moment. Upon forming the complex, there will be a certain amount of electron density that will presumably transfer from the proton acceptor to the donor molecule, as occurs in conventional H-bonds. In addition, there will be rearrangement of density within the confines of each monomer, usually thought of as internal polarization. Together, these effects will cause the dipole moment of the complex to differ from a simple vector sum of the moments of the two monomers, which would be the result of no density shift at all. This difference, along the direction of the C—H...O axis, is reported in Table 6 as $\Delta\mu_z$.

The increases observed in the moments are consistent with a certain amount of electron density shift from the proton acceptor molecule to the donor, much as occurs with conventional H-bonds. There is a clear correlation between stronger interaction energies and larger dipole enhancements. That is, $\Delta\mu_z$ rises in the sequence H₃CH < FH₂CH < F₂HCH < F₃CH. In the case of F₃CH...OH₂, $\Delta\mu_z$ is 0.405 D, nearly identical to the same quantity in the water dimer, even though the interaction energy of the former is weaker than that of the latter by 1 kcal/mol. This comparison indicates that the electron cloud in the C—H...O interaction is at least as mobile as the standard H-bond. In fact, $\Delta\mu_z$ is particularly large for both F₂HCH...OHCH₃ and F₂HCH...OCH₂ and their corresponding F₃CH analogues, where it surpasses the same quantity in the water dimer, with its stronger conventional H-bond. With regard to the various proton acceptors, $\Delta\mu_z$ follows the pattern OH₂ < H₂CO < CH₃OH. Comparison of this trend with that for interaction energies (H₂CO < OH₂ < CH₃OH) suggests that CH₃OH may owe some of its larger interaction energy to the greater polarizability attributed to the methyl group. While $\Delta\mu_z$ is larger for H₂CO than for OH₂, this enhanced polarizability is unable to make the former a stronger proton acceptor than is water in an energetic sense.

Whereas the dipole change reflects the overall shifts of electron density throughout the entire complex, one would like an estimate as to what fraction of this shift is internal as compared to the amount of density that transfers from one molecule to the other. A measure of the latter transfer arises by summing the atomic charges on one molecule or the other. Since the sum of these charges is zero in the isolated monomer, its magnitude in the complex is an estimate of the amount of density that shifts from one molecule to the other. These charge transfers are reported in the right half of Table 6, where they may be seen to be rather small, less than 15 me. As in the case of the dipole moment enhancements, the charge transfer becomes progressively larger as the proton donor is strengthened by F substitution. The carbonyl-containing H₂CO molecule loses less

Table 7. Change in Natural Population Atomic Charge (me) of Atoms in Complex Relative to Monomers^{74,a}

	Δq_H			Δq_C			Δq_O		
	OH ₂	CH ₃ -OH	H ₂ CO	OH ₂	CH ₃ -OH	H ₂ CO	OH ₂	CH ₃ -OH	H ₂ CO
H ₃ CH...	23	22	16	-7	-8	-4	-2	-1	-3
FH ₂ CH...	26	26	19	-9	-10	-6	-5	-5	-10
F ₂ HCH...	29	30	22	-13	-15	-9	-9	-10	-16
F ₃ CH...	32	33	25	-20	-22	-15	-12	-15	-23
HOH...	19			-24			-18		

^a Results were computed at the MP2/6-31+G** level.

net electron density than do OH₂ and CH₃OH, with their hydroxyl groups. The stronger binding of the water dimer results in a proportionately greater amount of charge transfer than in the CH...O cases, with the single exception of F₃CH...OHCH₃.

Comparison of the trends in the left and right parts of Table 6 leads to the following set of inferences. Both internal polarization of the monomers and charge transfer from one molecule to the other are roughly proportional to the strength of the proton donor. Adding a methyl group to water does not affect the charge transfer much, so the larger values of $\Delta\mu_z$ for CH₃OH are likely due to a greater degree of internal polarization. Likewise, since the charge transfer for the carbonyl acceptor is smaller than that for hydroxyl, H₂CO may be assumed to be more polarizable than the single bonds of OH₂.

The density shifts may also be quantified by considering the charges on individual atoms. While such charges are known to be sensitive to the particular basis set and the specific method of density partitioning, the *change* undergone by the charge of each atom, as the result of a particular chemical process, is typically both informative and insensitive to details of the means of its calculation. Table 7 lists the change in natural atomic charge⁷⁴ (in millielectrons) of each of the atoms of the C—H...O triad as a result of the formation of the indicated complex. It is first clear that the bridging H atom in the leftmost section of the table becomes more positive, while the C and O atoms both acquire more negative charge. This trend is consistent with the conventional H-bond contained in the water dimer, as indicated by the last entry in each section of data in Table 7. The principal distinction resides in the bridging H atom. Whereas the charge changes of the proton donor and acceptor atoms are larger in magnitude for the water dimer than for the weaker C—H...O interactions, the H atom shows a disproportionately large gain in positive charge in the latter cases, larger than in the water dimer. This larger charge increase ought to make this hydrogen more attractive toward the negatively charged O atom on the proton acceptor molecule.

The patterns of charge changes are consistent with those of the dipole moment enhancements and charge transfers in Table 6 in that the quantities are enhanced as the proton donor becomes stronger (H₃CH < FH₂CH < F₂HCH < F₃CH). There is little to distinguish proton acceptor OH₂ from CH₃OH, in terms of either charge transfer or atomic charge changes, so the greater dipole changes of Table 6 can be attributed to polarization of the methyl group of the latter and not to the primary C—H...O atoms. It is intriguing to note that the charge of the O atom of H₂CO is more susceptible to complexation than those in OH₂ and CH₃OH, while the H and C atoms of the donor molecules are affected *less* by complexation with H₂CO than with OH₂ or CH₃OH. Thus, the greater polarizability of H₂CO vs OH₂ is concentrated at its O atom.

Last, there has been some question as to whether the electrostatic attraction of the C—H...O interaction can be thought to occur between a negative O atom of the acceptor and either

a positively charged (CH) unit or a ${}^{-}\text{C}-\text{H}^{+}$ dipole.⁹⁰ It is interesting to note, in this regard, that there is no simple answer that characterizes the range of complexes considered here. That is, while the H atom bears a small positive charge in all monomers, the natural charge of the C atom in H_3CH , FH_2CH , F_2HCH , and F_3CH is respectively -0.915 , -0.168 , $+0.436$, and $+0.944$, covering a wide range and reversing sign. It would hence be oversimplistic to claim that the C atom is always positive or negative in these sorts of interactions. Another hypothesis that has been raised is that this sort of interaction might reverse the normal direction of the dipole from ${}^{+}\text{C}-\text{H}^{-}$ in the monomer to ${}^{-}\text{C}-\text{H}^{+}$.⁹¹ Our data would argue against this idea since (i) the charge on H is positive, even in the isolated monomers, and (ii) the small changes in C charge indicated in Table 7 could not cause such a reversal in its sign. One might also suspect that the greater bond dipole of O-H as compared to that of C-H would enable the conventional H-bond to polarize the proton acceptor molecule more than would be the case for a C-H...O interaction.⁸⁶ This idea is supported by the larger increase of negative charge on the proton-accepting O atom of OH_2 for the water dimer (18 me) than for the other cases.

Any scheme of assigning charge to the various nuclei is subject to a certain degree of arbitrariness. For this reason, it is often helpful to complement the charge data with plots that map out shifts of electron density throughout the entire region of the complex. Such maps are provided in Figure 4, where the dark and light regions indicate loss and gain of electron density, respectively. Figure 4a-c refers to the CH...O interaction between water as proton acceptor and H_3CH , FH_2CH , and F_2HCH as donor, respectively. Despite the range of the strength of the interaction for these three complexes, and the optimized intermolecular distances which span a range between 3.59 and 3.34 Å, the plots are remarkably similar. In each case, the water molecule occupies a region of density loss, more or less centered on the O atom. Moving from right to left, toward the bridging H atom, one first encounters a region of charge gain and then loss. The latter region sits rather close to the hydrogen nucleus and is consistent with the enhancements in this atom's positive charge in Table 7.

There are other features that emerge as the interaction strengthens and as the two molecules come closer together. A region of charge gain appears on the far side of the proton acceptor molecule, which develops additional structure as one goes from a to b to c in Figure 4. There is also some development of regions of density gain in the vicinity of the bridging hydrogen, primarily off the CH...O axis. There is a perhaps surprisingly small amount of charge shift visible within the confines of the proton donor molecule, whether it be H_3CH , FH_2CH , or F_2HCH . The patterns of density shift in Figure 4 are altered very little if the proton acceptor is changed from OH_2 to H_2CO or CH_3OH .

It is of interest to compare these charge shift patterns with those that occur in a conventional H-bond. There is one complication, however, in that the H-bond length in the water dimer is about 0.5 Å shorter than those in these CH...O systems. To be as consistent as possible in the comparison, we first illustrate the density shifts of the water dimer in Figure 5a, where the interoxygen separation is taken as 3.592 Å, the equilibrium $R(\text{CH}\cdots\text{O})$ in the $\text{H}_3\text{CH}\cdots\text{OH}_2$ complex. The patterns in Figure 5a are basically similar to those in Figure 4, with a few

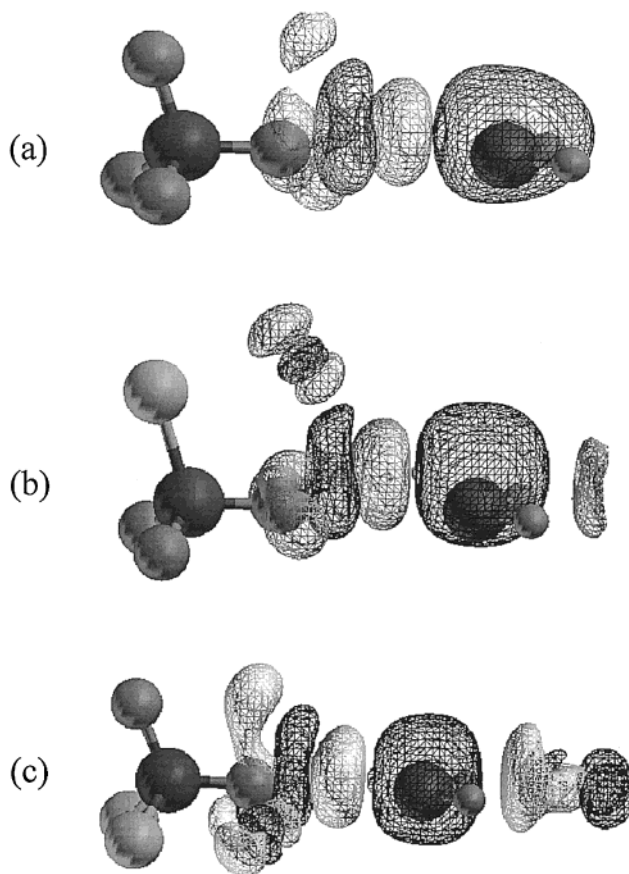


Figure 4. Density difference maps for $\text{F}_n\text{H}_{3-n}\text{CH}\cdots\text{OH}_2$ for (a) $n = 0$, (b) $n = 1$, and (c) $n = 2$, all in linear geometry ($\alpha = 0$, $\beta = 180^\circ$), at optimum values of R . Dark regions represent loss of electron density as a result of formation of the complex, relative to isolated monomers; light regions refer to increased density. The contour shown is 0.0005 e/au^3 , calculated at the MP2/6-31+G** level.

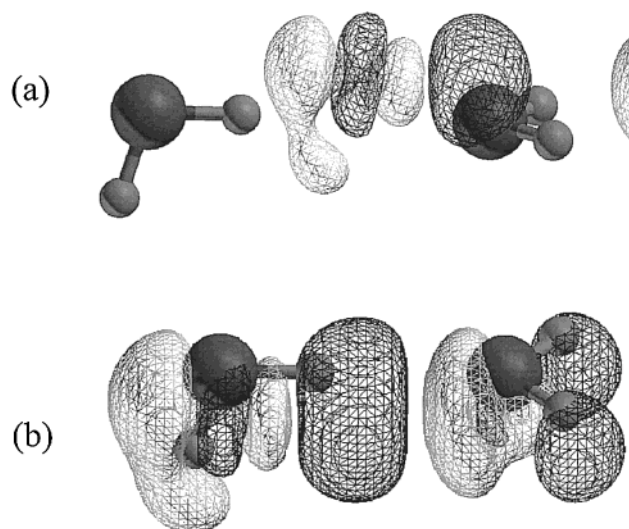


Figure 5. Density difference maps for water dimer in linear geometry ($\alpha = 0$, $\beta = 180^\circ$). Dark regions represent loss of electron density as a result of formation of the complex, relative to isolated monomers; light regions refer to increased density. The contour shown is 0.0005 e/au^3 , calculated at the MP2/6-31+G** level. R is equal to the optimized value in $\text{H}_3\text{CH}\cdots\text{OH}_2$ in (a) and equal to its optimized value in the water dimer in (b).

exceptions. In the first place, there is an extra region of charge gain which is added to the H-bond axis for the water dimer. Like the CH...O systems, the proton acceptor atom lies in a

(90) Starikov, E. B.; Steiner, T. *Acta Crystallogr.* **1997**, *D53*, 345.

(91) Wiberg, K. B.; Waldron, R. F.; Schulte, G.; Saunders, M. *J. Am. Chem. Soc.* **1991**, *113*, 971.

Table 8. Morokuma Partitioning of Contributions to Complexation Energy (kcal/mol)^a

	ES			EX			POL			CT			CORR		
	OH ₂	CH ₃ OH	H ₂ CO	OH ₂	CH ₃ OH	H ₂ CO	OH ₂	CH ₃ OH	H ₂ CO	OH ₂	CH ₃ OH	H ₂ CO	OH ₂	CH ₃ OH	H ₂ CO
H ₃ CH···	-0.42	-0.39	-0.23	0.38	0.33	0.18	-0.13	-0.12	-0.08	-0.11	-0.12	-0.08	-0.08	-0.21	-0.21
FH ₂ CH···	-1.96	-1.91	-1.40	1.17	1.16	0.62	-0.24	-0.25	-0.16	-0.32	-0.35	-0.21	-0.20	-0.33	-0.18
F ₂ HCH···	-3.83	-3.85	-2.74	2.06	2.14	1.15	-0.36	-0.43	-0.28	-0.53	-0.60	-0.35	-0.25	-0.46	-0.10
F ₃ CH···	-7.06	-7.50	-5.15	4.14	4.74	2.40	-0.69	-0.97	-0.61	-0.97	-1.16	-0.63	-0.25	-0.51	0.05
HOH···	-7.58			4.24			-0.71			-0.93			-0.30		

^a Results were computed with the 6-31+G** basis set.

region of charge loss, and as one moves to the left toward the bridging hydrogen, there is first encountered a region of gain and then loss again. For the water dimer in Figure 5a, a new region of charge gain occurs before the bridging H atom is reached.

On the other hand, this extra region may not be characteristic of conventional H-bonds but is rather an artifact of the artificially long length in Figure 5a. When the two water molecules are allowed to move closer, to their equilibrium separation of 2.927 Å as in Figure 5b, it may be seen that the four regions of charge loss/gain in Figure 5a collapse into just two. The stronger molecular interaction also leads to the development of more regions of loss and gain that become visible at the 0.0005 e/au³ contour chosen for purposes of illustration in these figures. One can conclude that the charge density difference maps do not reveal any fundamental differences between CH···O and conventional H-bonds, other than distinctions which appear to be connected with the different equilibrium separations in the two sorts of systems.

Energy Decomposition Analysis. Deeper insights into the fundamental character of the C–H···O interaction may be gleaned from a decomposition of the total interaction energy into its component parts. There are a variety of ways in which this can be done, but the scheme which has received the most use over the years is that of Morokuma and co-workers.⁹² Briefly, the interaction is envisioned as occurring in two stages. The two molecules are first brought together, but without allowing their interaction to modify the electronic distribution of each monomer. The Coulombic interaction between these frozen charge distributions is dubbed the electrostatic (ES) term; the exchange energy (EX) is associated with the steric repulsions that arise from the overlap of the monomer charge clouds. In the second stage, the charge clouds of the two monomers are allowed to respond to the interaction. The shifts of electron density that occur within one monomer or the other are denoted the polarization energy (POL), while charge transfer (CT) occurs when the electron density of one molecule is shifted into the space of its partner. (A last term, known as mixing (MIX), arises from the failure of the above four terms to fully account for all aspects of the interaction.) Note that this list does not include dispersion, which is a phenomenon associated with electron correlation; an estimate of dispersion energy, similar in spirit to London forces, can be gained from the correlation contributions to the interaction energies, reported in the last section of Table 8 as CORR, the difference in binding energy between the MP2 and SCF levels.

The Morokuma components of the interaction energies of the various complexes, calculated with the aid of the GAMESS program,⁹³ are displayed in Table 8, along with comparable data

(92) Morokuma, K.; Kitaura, K. In *Molecular Interactions*; Ratajczak, H., Orville-Thomas, W. J., Eds.; Wiley: New York, 1980; Vol. 1, p 21.

(93) Schmidt, M. W.; Baldridge, K. K.; Boatz, J. A.; Elbert, S. T.; Gordon, M. S.; Jensen, J. H.; Koseki, S.; Matsunaga, N.; Nguyen, K. A.; Su, S.; Windus, T. L.; Dupuis, M.; Montgomery, J. A. *J. Comput. Chem.* **1993**, *14*, 1347.

for the O–H···O H-bond of the water dimer. As anticipated, all of the components are attractive (negative in sign), with the exception of the exchange repulsion. For most components, there is a clear progression toward larger magnitude down a column, as the proton donor is strengthened. With regard to the proton acceptor, the first four of the components are uniformly smaller for H₂CO than for either OH₂ or CH₃OH. The latter two acceptors are virtually indistinguishable from one another, although there is a trend for the components to be larger for CH₃OH than for OH₂, when paired with F₂HCH or F₃CH. The correlation component, on the other hand, is consistently and substantially larger for CH₃OH than for OH₂, suggesting that the slightly greater interaction energies connected with the former are due, in large part, to a greater dispersion energy, probably due, in turn, to its larger size.

Unlike the other two proton acceptors, the correlation term for H₂CO shows a curious pattern of diminishing contribution with stronger proton donors. This lowered attraction is likely due to the fact that, unlike OH₂ or CH₃OH, the MP2 dipole moment of H₂CO is some 12% smaller than its SCF moment. The lower moment leads to a reduced electrostatic attraction at the MP2 level, an apparent repulsive contributor to CORR,⁹⁴ which detracts from the attractive dispersion energy. This effect grows proportionately with the magnitude of the ES term itself, making CORR progressively less negative as the donor becomes more polar.

The similarity between the trends in the charge-transfer components of the interaction energies in Table 8 and the amount of electron density transferred from proton acceptor to donor in Table 6 serves as verification of both quantities. In either case, the quantity grows in the order H₃CH < FH₂CH < F₂HCH < F₃CH. Further, there is little distinction between acceptors OH₂ and CH₃OH, both of which are larger than the values for H₂CO.

Inspection of the data in the last row of Table 8 reiterates the generally accepted notion that the conventional H-bond is largely electrostatic in origin, with much smaller attractive contributions from polarization, charge transfer, and dispersion. Exchange repulsion is comparable, although smaller in magnitude, to ES, and of opposite sign. Precisely the same statements may be made about the C–H···O interactions. In fact, the similarities extend to a quantitative analysis. For example, the POL and CT components amount to 9 and 12%, respectively, of the ES term in the water dimer; the same ratios are 9 and 14% in the F₂HCH···OH₂ complex and 10 and 14% in F₃CH···OH₂.

The aforementioned contractions of the C–H bond in these CH···O complexes are particularly intriguing, opposite as they are to the stretches observed in conventional H-bonds. Indeed, this particular opposite behavior has led one research group to label such CH···O interactions as “anti-H-bonds”,⁵⁸ so more detailed examination via energy decomposition is clearly

(94) Szczesniak, M. M.; Scheiner, S. *J. Chem. Phys.* **1986**, *84*, 6328.

Table 9. Effects on Morokuma Components (kcal/mol) to Complexation Energy of Stretching XH (X = C, O) Bond^a

	F ₂ HCH...OH ₂	HOH...OH ₂
ES	-0.07	-0.20
EX	+0.13	+0.22
POL	-0.01	-0.03
CT	-0.03	-0.07
MIX	+0.01	+0.02
CORR	-0.02	-0.02
total	+0.01	-0.08

^a Results were computed with the 6-31+G** basis set. Results are for the total stretch of 0.010 Å, from 0.005 Å shorter than equilibrium value in isolated monomer to 0.005 Å longer.

warranted. The first column of Table 9 reports the change in each component that arises when the C–H bond in F₂HCH...OH₂ is stretched by a total of 0.010 Å. (More specifically, the reference point for this stretch is the equilibrium C–H bond length in the isolated F₂HCH molecule.) The second column of data in Table 9 represents the corresponding data for the O–H bond in the water dimer, with its conventional OH...O H-bond.

The negative signs of the entries in the first row of Table 9 indicate that the electrostatic interaction favors a bond stretch. That is, ES becomes more attractive when either the CH or the OH bond is elongated. This trend is more pronounced in the case of the water dimer, but this larger value is mainly due to the closer proximity of the two subunits, which enhances the effect. The stretch of either bond increases the exchange repulsion, consistent with the greater overlap of the electron clouds of the proton acceptor water and the approaching hydrogen. The greater sensitivity of EX in the water dimer is again due to the smaller intermolecular separation. Although smaller in magnitude than ES, the POL and CT components likewise favor a stretch of the bond. Consistent with the aforementioned insensitivity of the CH or OH bond length to correlation, the correlation contributions to the energy needed to stretch these bonds can be seen to be quite small in Table 9. In summary, all the various components to the stretching energy in the CH...O and OH...O systems are identical in sign, suggesting that very similar forces are in effect in each case. The two systems differ only in the magnitudes of these forces, which are larger in the OH...O case due to the closer proximity of the two subunits.

The final row of Table 9 sums the various components to the stretching energy. The positive value for F₂HCH...OH₂, suggesting a rise in total energy as the bond is stretched, is consistent with the contraction of this bond in the complex, just as the negative value for the total in HOH...OH₂ indicates the stretch that this bond undergoes. Perhaps most important is the observation that the total is of small magnitude, resulting from large-scale cancellations. There are several inferences one might draw from Table 9. For example, one may attribute the OH stretch in the water dimer to a large electrostatic push in this direction. It would be equally valid to note that the ES and EX components nearly cancel one another and to thus claim that the stretch is attributable, instead, to the POL and CT components.

In any case, the central question here is, why does the CH bond contract? One could attribute this, perhaps, to a smaller ES tendency for the CH bond to stretch, which is more easily overcome by the exchange pressure toward a shorter bond. A second interpretation might place the blame on the smaller POL and CT trends toward a longer bond, as compared to OH...O. But of perhaps greatest importance is the observation that the trends in all of the components in the CH...O and OH...O cases

are identical. Thus, the fact that the CH bond contracts while the OH bond elongates in the complexes does not represent any fundamental difference between the two types of interactions but reflects merely the less profound result that the forces pushing toward contraction in one case are slightly larger than the elongation forces, while the opposite is true in the other case.

A previous theoretical study noted that the dipole moment of a proton donor molecule such as F₃CH is lowered when the CH bond stretches.⁵⁸ Indeed, our calculations verify that this same phenomenon is characteristic of related molecules, in that the moment of the entire set of F_nH_{3-n}CH all diminish as the CH bond is elongated. In more quantitative terms, the linear relation between dipole moment and CH bond length over a short range indicates that a stretch of 10 mÅ in this bond will lower the dipole moment between 0.004 and 0.009 D.

The earlier authors⁵⁸ had taken this dipole reduction as evidence that the electrostatic attraction between the proton donor and acceptor would likewise be diminished by the CH bond stretch. However, this contention is based on two faulty premises. In the first place, the total electrostatic attraction includes not only the dipole–dipole interaction, which is the basis of the earlier argument, but also a number of other terms, e.g., quadrupole–dipole or quadrupole–quadrupole, that are independent of the dipole moment of the proton donor. Second, at the relatively short intermolecular separations within these complexes, the multipole approximation by which the electrostatic interaction is partitioned into separable terms is itself questionable and possibly divergent. Indeed, the negative value for the ES term for the F₂HCH...OH₂ system in Table 9 confirms the error in equating the total electrostatic interaction simply with the magnitude of the dipole moment of the proton donor. Whereas the dipole moment of F₂HCH is lowered by the stretch of its CH bond, this elongation nevertheless produces an enhancement of the electrostatic attraction between F₂HCH and OH₂.

Of course, there is no doubt that the diminished moment of F₂HCH reduces the amount of ES stabilization over what it would be if the moment were to increase. The lowered moment is likely one reason that the ES stabilization for F₂HCH...OH₂ is only -0.07 kcal/mol, much smaller in magnitude than the -0.20 kcal/mol observed in the water dimer, where the moment of the proton donor molecule is increased by the stretch of the OH bond. Hence, the opposite effect of a CH bond stretch upon the monomer's molecular moment, as compared to an OH bond, certainly contributes to the observation of a contraction in the CH...O case and stretch in OH...O. Our central point here is that the ES components of the interaction energies of the CH...O and OH...O systems are *both* stabilized by a stretch of the bond. When coupled to the observation that all of the components of the interaction energy behave in a qualitatively similar way for the two types of H-bonds, it is difficult to conclude that there is any profound or fundamental difference between the CH...O and OH...O interactions, nor are there sufficient grounds to label the former as an "anti-H-bond".

Conclusions

C–H...O interactions appear to be very similar to conventional H-bonds in most respects, albeit generally weaker. A hydrocarbon such as CH₄ forms a very weak interaction with a proton acceptor such as water, with a binding energy of only a fraction of a kilocalorie per mole. The two subunits are far apart in their equilibrium geometry, separated by a R(C...O) distance of more than 3.5 Å. However, the interaction is strengthened

as electronegative substituents such as fluorine are added to the hydrocarbon. Each F atom adds about 1 kcal/mol to the binding energy and draws the two subunits closer together by some 0.10–0.15 Å. The strength of the interaction is much less sensitive to the nature of the proton acceptor than to the donor. Adding a methyl group to the water acceptor strengthens the binding by a small amount; most of this increment can be attributed to the enhanced dispersion that accompanies the larger acceptor molecule. The carbonyl oxygen of H₂CO is a slightly poorer proton acceptor in these C–H···O interactions.

Hydrogen bonds which incorporate CH proton donors have much the same sensitivity to distortions from their equilibrium geometry as do conventional H-bonds. Both C–H···O and O–H···O are disposed toward a linear arrangement of these three atoms, although the former can be more easily bent. With regard to orientation around the proton acceptor molecule, the two sorts of interactions behave essentially identically with one another. One difference of some significance is that, while the C–H···O bonds are weaker than conventional H-bonds, their binding energy dies off more gradually as the distance between the two subunits is stretched. This observation leads to the possibility of a situation where a C–H···O bond may, in fact, be stronger than a corresponding O–H···O interaction at a particular intermolecular separation.

Another point of strong similarity between C–H···O and O–H···O interactions lies within the redistributions of electron density that accompany their formation. In either case, stronger interactions lead to progressively larger shifts of density which manifest themselves in a number of ways. The amount of charge transferred from one molecule to the other is roughly proportional to the binding strength, as is the dipole moment enhancement. The trends of charge gain and loss on the pertinent atoms are quite similar for the two sorts of H-bonds, as are the patterns that appear in detailed maps of density shift that encompass the entire complex. The only significant difference lies in the fact that the bridging H atom appears to become somewhat more positive as a result of C–H···O interaction than it does in the case of O–H···O.

Prior decomposition of the binding energy of a conventional H-bond had revealed that the electrostatic attraction is the largest contributor, much more so than the components associated with charge transfer, polarization, or dispersion. These attractive forces are all opposed by the exchange/steric repulsion between the electron clouds of the two subunits, which is smaller in magnitude than the electrostatic component. Precisely the same trends are observed in the C–H···O bond, further adding to

the evidence that it is fundamentally very similar to a conventional H-bond.

The only significant aspect in which the C–H···O and O–H···O interactions are found to differ revolves around the change in the length of the CH (OH) bond that occurs upon formation of the H-bond. Whereas the OH bond of conventional H-bonds is known to stretch, and its vibrational frequency is known to undergo a red shift and accompanying intensification, the CH bond suffers precisely opposite changes. Indeed, the CH contraction is enhanced as the C–H···O bond is strengthened, as is the amount of its blue shift. Detailed scrutiny reveals that this opposite behavior is *not* indicative of any fundamental distinction between the two sorts of H-bonds. The change in XH bond length is the net resultant of one set of forces tending toward elongation and another that pulls toward a shorter bond. These same forces are in operation in both types of H-bond: electrostatic, polarization, charge transfer, and dispersion push the hydrogen away from the donor atom, while exchange pulls it away from the acceptor. While the former set are together slightly stronger than the exchange for a O–H···O bond, the latter very narrowly overcomes the former set in the C–H···O case. The red (blue) shift in the O–H···O (C–H···O) bond then follows naturally from this bond stretch (contraction).

In summary, then, the calculations reported here support the notion that C–H···O interactions can be categorized as true H-bonds, although they of course tend to be weaker due to the normally lesser proton donating ability of C as compared to that of O.

Acknowledgment. This work was supported by NIH Grant GM57936. S.S. acknowledges a Summer Research Fellowship from Southern Illinois University.

Note Added in Proof: Cubero et al.⁹⁵ have recently examined interactions between various CH donors and benzene as the acceptor. Consistent with our results reported above, CH donors with sp³ hybridization show a bond contraction and blue shift, whereas a stretch and red shift are observed for sp donors such as HCCH and HCN. More importantly, the topology of the electron density appears to be essentially the same, regardless of whether the CH bond stretches or contracts, in line with our conclusion of no fundamental difference between CH and conventional H-bonds.

JA991795G

(95) Cubero, E.; Orozco, M.; Hobza, P.; Luque, F. J. *J. Phys. Chem. A* **1999**, *103*, 6394.